

Generalized Category Discovery

Sagar Vaze*

Kai Han†

Andrea Vedaldi*

Andrew Zisserman*

*Visual Geometry Group, University of Oxford

†The University of Hong Kong

{sagar, vedaldi, az}@robots.ox.ac.uk

kaihanx@hku.hk

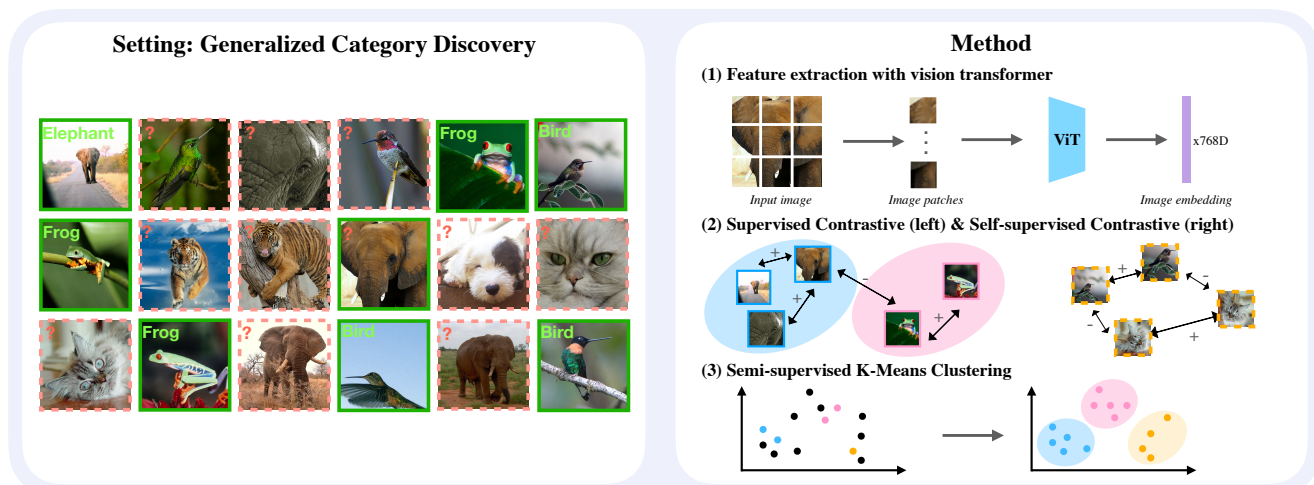


Figure 1. We present a new setting: ‘Generalized Category Discovery’ and a method to tackle it. Our setting can be succinctly described as: given a dataset, a subset of which has class labels, categorize all unlabelled images in the dataset. Our method leverages the properties of contrastively trained vision transformers to assign labels directly through clustering.

Abstract

In this paper, we consider a highly general image recognition setting wherein, given a labelled and unlabelled set of images, the task is to categorize all images in the unlabelled set. Here, the unlabelled images may come from labelled classes or from novel ones. Existing recognition methods are not able to deal with this setting, because they make several restrictive assumptions, such as the unlabelled instances only coming from known — or unknown — classes and the number of unknown classes being known *a-priori*. We address the more unconstrained setting, naming it ‘Generalized Category Discovery’, and challenge all these assumptions. We first establish strong baselines by taking state-of-the-art algorithms from novel category discovery and adapting them for this task. Next, we propose the use of vision transformers with contrastive representation learning for this open world setting. We then introduce a simple yet effective semi-supervised *k*-means method to cluster the unlabelled data into seen and unseen classes automatically, substantially outperforming the

baselines. Finally, we also propose a new approach to estimate the number of classes in the unlabelled data. We thoroughly evaluate our approach on public datasets for generic object classification including CIFAR10, CIFAR100 and ImageNet-100, and for fine-grained visual recognition including CUB, Stanford Cars and Herbarium19, benchmarking on this new setting to foster future research. Code: github.com/sgvaze/generalized-category-discovery

1. Introduction

Consider an infant sitting in a car and observing the world. Object instances will pass the car and, for some of these, the infant may have been told their category (‘that is a dog’, ‘that is a car’) and be able to recognize them. There will also be instances that the infant has not seen before (cats and bicycles) and, having seen a number of these instances, we might expect the infant’s visual recognition system to cluster these into new categories.

This is the problem that we consider in this work: given an image dataset where only some images are labelled with

their category, assign a category label to all other images, possibly using new categories not observed in the labelled set. We term this problem *Generalized Category Discovery* (GCD), and suggest that this is a realistic use case for many machine vision applications: whether that is recognizing products in a supermarket; pathologies in medical images; or vehicles in autonomous driving.

To motivate this problem, consider the limitations of existing image recognition settings. In image classification, one of the the most widely studied problems, all of the training images come with class labels. Furthermore, all images at test time come from the same classes as the training set. Semi-supervised learning (SSL) [6] introduces the problem of learning from unlabelled data, but still assumes that all unlabelled images come from the same set of classes as the labelled ones. More recently, the tasks of open-set recognition (OSR) [35] and novel-category discovery (NCD) [17] have tackled open-world settings in which the images at test time may belong to new classes. However, OSR aims only to *detect* test-time images which do not belong to one of the classes in the labelled set, but does not require any further classification amongst these detected images. Meanwhile, in NCD, the closest setting to the one tackled in this work, methods learn from labelled and unlabelled images, and aim to discover new classes in the unlabelled set. However, NCD still makes the limiting assumption that *all* of the unlabelled images come from new categories, which is usually unrealistic.

In this paper, we tackle Generalized Category Discovery in a number of ways. Firstly, we establish strong baselines by taking representative methods from NCD and applying them to this task. To do this, we adapt their training and inference mechanisms to account for our more general setting, as well as retrain them with a more robust backbone architecture. We show that existing NCD methods are prone to overfit the labelled classes in this generalized setting.

Next, observing the potential for NCD methods to overfit their classification heads to the labelled classes, we propose a simple but effective method for recognition by clustering. Our key insight is to leverage the strong ‘nearest neighbour’ classification property of vision transformers along with contrastive learning. We propose the use of contrastive training and a semi-supervised k -means clustering algorithm to recognize images without a parametric classifier. We show that these proposed methods substantially outperform the established baselines, both on generic object recognition datasets and, particularly, on more challenging fine-grained benchmarks.

Finally, we propose a solution to a challenging and under-investigated problem in image recognition: estimating the number of categories in unlabelled data. Almost all methods, including purely unsupervised ones, assume the knowledge of the number of categories, a highly unrealistic

assumption in the the real world. We propose an algorithm which leverages the labelled set to tackle this problem.

Our contributions can be summarized as follows:

- The formalization of Generalized Category Discovery (GCD), a new setting for image recognition.
- The establishment of strong baselines by transferring and adapting state-of-the-art techniques from standard novel category discovery to this task.
- A simple but effective method for GCD, which uses contrastive representation learning and clustering to directly provide class labels, and outperforms the baselines substantially.
- A novel method for estimating the number of categories in unlabelled data, a largely understudied problem.

We hope that this paper will serve as a springboard for future work on this more realistic version of open world image recognition.

2. Related work

Our work relates to prior work on *semi-supervised learning*, *open-set recognition*, and *novel category discovery*, which we briefly review next.

Semi-supervised learning. A vast number of methods [6, 30, 34, 37, 46] have been proposed to tackle the problem of semi-supervised learning (SSL). SSL assumes that the labelled and unlabelled instances are from the same set of classes. The objective is to learn a robust classification model leveraging both the labelled and unlabelled data during training. Amongst existing methods, the consistency based approaches appear to be popular and effective, such as LadderNet [33], PI model [27], Mean-teacher [40]. Recently, with the success of self-supervised learning, methods have also been proposed to improve SSL by augmenting the methods with self-supervised objectives [34, 46].

Open-set recognition. The problem of open-set recognition (OSR) is formalized in [35], with the objective being to classify unlabelled instances from the same semantic classes as the labelled data, while identifying unlabelled instances from unseen classes. OpenMax [3] is the first deep learning method to approach this problem with Extreme Value Theory. GANs are often employed to generate adversarial samples to train the open-set classifier, e.g., [13, 23, 29]. Several methods have been proposed to train models such that images with large reconstruction error are regarded as open-set samples [31, 38, 45]. There are also methods that learn prototypes for the labelled classes, and identify the images from unknown classes by the distances to the prototypes [7, 8, 36]. More recently, [7, 8] proposed to learn the reciprocal points which describe ‘otherness’ with respect to the labelled classes. [47] jointly trains a flow-based density estimator and a classification based encoder

for OSR. Finally, Vaze et al. [42] study the correlation between closed-set and open-set performance, and show that state-of-the-art OSR results can be obtained by boosting the closed-set performance on the cross-entropy baseline.

Novel category discovery. The problem of novel category discovery (NCD) is formalized in DTC [17]. Earlier methods that can be applied to this problem are KCL [19] and MCL [20], both of which maintain two models trained with labelled data and unlabelled data respectively, for general task transfer learning. AutoNovel (aka Rankstats) [15, 16] tackles the NCD problem with a three stage method. The model is firstly trained with self-supervision on all data for low-level representation learning. Then, it is further trained with full supervision on labelled data to capture higher level semantic information. Finally, a joint learning stage is carried out to transfer knowledge from the labelled to unlabelled data with ranking statistics. Zhao and Han [48] propose a model with two branches, one for global feature learning and the other for local feature learning, such that dual ranking statistics and mutual learning are conducted with these two branches for better representation learning and new class discovery. OpenMix [50] mixes the labelled and unlabelled data to avoid the model from over-fitting for NCD. NCL [49] extracts and aggregates the pairwise pseudo-labels for the unlabelled data with contrastive learning and generates hard negatives by mixing the labelled and unlabelled data in the feature space for NCD. Jia et al. [21] propose an end-to-end NCD method for single- and multi-modal data with contrastive learning and winner-takes-all hashing. A unified cross-entropy loss is introduced in UNO [12] to allow the model to be trained on labelled and unlabelled data jointly by swapping the pseudo-labels from labelled and unlabelled classification heads.

3. Generalized category discovery

We first formalize the task of *Generalized Category Discovery* (GCD). In short, we consider the problem of classifying images in a dataset, a subset of which has known class labels. The task is to assign class labels to all remaining images, using classes that may or may not be observed in the labelled images (see Fig. 1, left).

Formally, we define GCD as follows. We consider a dataset \mathcal{D} comprising two parts $\mathcal{D}_{\mathcal{L}} = \{(\mathbf{x}_i, y_i)\}_{i=1}^N \in \mathcal{X} \times \mathcal{Y}_{\mathcal{L}}$ and $\mathcal{D}_{\mathcal{U}} = \{(\mathbf{x}_i, y_i)\}_{i=1}^M \in \mathcal{X} \times \mathcal{Y}_{\mathcal{U}}$, where $\mathcal{Y}_{\mathcal{L}} \subset \mathcal{Y}_{\mathcal{U}}$. During training, the model does not have access to the labels in $\mathcal{D}_{\mathcal{U}}$, and is tasked with predicting them at test time. Furthermore, we assume access to a validation set, $\mathcal{D}_{\mathcal{V}} = \{(\mathbf{x}_i, y_i)\}_{i=1}^{N'} \in \mathcal{X} \times \mathcal{Y}_{\mathcal{L}}$, which is disjoint from the training set and contains images from the same classes as the labelled set. This formalization allows us to clearly see the distinction with the novel category discovery setting. NCD assumes $\mathcal{Y}_{\mathcal{L}} \cap \mathcal{Y}_{\mathcal{U}} = \emptyset$ and existing methods use this prior knowledge during training.

In this section, we describe the methods we propose in order to tackle GCD. We begin by describing our approach to the problem. Leveraging recent progress in self-supervised representation learning, we propose a simple but effective approach based on contrastive learning, with classification labels provided by a semi-supervised k -means algorithm. Next, we develop a method to estimate the number of categories in the unlabelled data, which is a challenging task that is understudied in the literature. Finally, we build two strong baselines for this problem by modifying state-of-the-art NCD methods, RankStats [16] and UNO [12], to fit with our setting.

3.1. Our approach

The key insight of our approach for image recognition in an open-world setting is to remove the need for parametric classification heads. Instead, we perform clustering directly in the feature space of a deep network (see Fig. 1, right). Classification heads (typically, linear classifiers on top of a learned embedding) are best trained with the cross-entropy loss, which has been shown to be susceptible to noisy labels [11]. Furthermore, when training a linear classifier for unlabelled classes, a typical method is to generate (noisy) pseudo-labels for the unlabelled instances. This would suggest that parametric heads are susceptible to performance deterioration on the unlabelled classes. Finally, we note that, by necessity, classification heads must be trained from scratch, which further makes them vulnerable to overfitting on the labelled classes.

Meanwhile, self-supervised contrastive learning has been widely used as pre-training to achieve robust representations in NCD [21, 49]. Furthermore, when combined with vision transformers, it generates models which are good nearest neighbour classifiers [5]. Inspired by this, we find that contrastively training a ViT model allows us to directly cluster in the model’s feature space, thereby removing the need for a linear head which could lead to overfitting. Specifically, we train the representation with a noise contrastive loss [14] on all images *without using any labels*. This is important because it avoids overfitting the features to the subset of classes that are (partially) labelled. We add a further supervised contrastive component [22] for the labelled instances to make use of the labelled data (see Fig. 1, middle row on the right).

3.1.1 Representation learning

We use, for all methods, a vision transformer (ViT-B-16) [10] pretrained with DINO [5] self-supervision on (unlabelled) ImageNet [9] as our backbone. This is motivated firstly because the DINO model is a strong nearest neighbour classifier, which suggests non-parametric clustering in its feature space would work well. Secondly, self-

supervised vision transformers have demonstrated the attractive quality of learning to attend to salient parts of an object without human annotation. We find this feature to be useful for this task, because *which* object parts are important for classification is likely to transfer well from the labelled to the unlabelled categories (see Sec. 4.5).

Finally, we wish to reflect a realistic and practical setting. In the NCD literature, it is standard to train a ResNet-18 [18] backbone from scratch for the target task. However, in a real-world setting, a model is often initialized with large-scale pretrained weights to optimize performance (often ImageNet supervised pretraining). In order to avoid conflicts with our experimental setting (which assumes a finite labelled set), we use self-supervised ImageNet weights. To enhance the representation such that it is more tailored for the labelled and unlabelled data we have, we further fine-tune the representation on our target data jointly with supervised contrastive learning on the labelled data, and unsupervised contrastive learning on *all* the data.

Formally, let \mathbf{x}_i and $\mathbf{x}_{i'}$ be two views (random augmentations) of the same image in a mini-batch B . The unsupervised contrastive loss is written as:

$$\mathcal{L}_i^u = -\log \frac{\exp(\mathbf{z}_i \cdot \mathbf{z}_{i'} / \tau)}{\sum_n \mathbb{1}_{[n \neq i]} \exp(\mathbf{z}_i \cdot \mathbf{z}_n / \tau)}, \quad (1)$$

where $\mathbf{z}_i = \phi(f(\mathbf{x}_i))$ and $\mathbb{1}_{[n \neq i]}$ is an indicator function evaluating to 1 *iff* $n \neq i$, and τ is a temperature value. f is the feature backbone, and ϕ is a multi-layer perceptron (MLP) projection head.

The supervised contrastive loss is written as:

$$\mathcal{L}_i^s = -\frac{1}{|\mathcal{N}(i)|} \sum_{q \in \mathcal{N}(i)} \log \frac{\exp(\mathbf{z}_i \cdot \mathbf{z}_q / \tau)}{\sum_n \mathbb{1}_{[n \neq i]} \exp(\mathbf{z}_i \cdot \mathbf{z}_n / \tau)}, \quad (2)$$

where $\mathcal{N}(i)$ denotes the indices of other images having the same label as \mathbf{x}_i in the mini-batch B . Finally, we construct the total loss over the batch as:

$$\mathcal{L}^t = (1 - \lambda) \sum_{i \in B} \mathcal{L}_i^u + \lambda \sum_{i \in B_{\mathcal{L}}} \mathcal{L}_i^s \quad (3)$$

where $B_{\mathcal{L}}$ corresponds to the labelled subset of B and λ is a weight coefficient. Using the labels *only* in a contrastive framework, rather than in a cross-entropy loss, means that unlabelled and labelled data are treated similarly. The supervised contrastive component is only used to nudge the network towards a semantically meaningful representation, thereby minimizing overfitting on the labelled classes.

3.1.2 Label assignment with semi-supervised k -means

Given the learned representation for the data, we can now assign class or cluster labels for each unlabelled data point,

either from the labelled classes or unseen new classes. Instead of performing this parametrically as is common in NCD (and risk overfitting to the labelled data) we propose to use a non-parametric method. Namely, we propose to modify the classic k -means into a constraint algorithm by forcing the assignment of the instances in $\mathcal{D}_{\mathcal{L}}$ to the correct cluster based on their ground-truth labels. Note, here we assume knowledge of the number of clusters, k . We tackle the problem of estimating this parameter in Sec. 3.2. The initial $|\mathcal{Y}_{\mathcal{L}}|$ centroids for $\mathcal{D}_{\mathcal{L}}$ are obtained based on the ground-truth class labels, and an additional $|\mathcal{Y}_{\mathcal{U}} \setminus \mathcal{Y}_{\mathcal{L}}|$ (number of new classes) initial centroids are obtained from $\mathcal{D}_{\mathcal{U}}$ with k -means++ [1], constrained on the centroids of $\mathcal{D}_{\mathcal{L}}$. During each centroid update and cluster assignment cycle, instances from the same class in $\mathcal{D}_{\mathcal{L}}$ are always forced to have the same cluster assignment, while each instance in $\mathcal{D}_{\mathcal{U}}$ can be assigned to any cluster based on the distance to different centroids. After the semi-supervised k -means converges, each instance in $\mathcal{D}_{\mathcal{U}}$ can be assigned a cluster label. We provide a clear diagram of this in Appendix B.

3.2. Estimating the class number in unlabelled data

Here, we tackle the problem of finding the number of classes in the unlabelled data. In the NCD and unsupervised clustering settings, prior knowledge of the number of categories in the dataset is assumed, but this is unrealistic in the real world given that the labels themselves are unknown. To estimate the number of categories in $\mathcal{D}_{\mathcal{U}}$, we leverage the information available in $\mathcal{D}_{\mathcal{L}}$. Specifically, we perform k -means clustering on the entire dataset, \mathcal{D} , before evaluating clustering accuracy on *only* the labelled subset (see Sec. 4.1 for the metric's definition).

Clustering accuracy is evaluated by running the Hungarian algorithm [26] to find the optimal assignment between the set of cluster indices and ground truth labels. If the number of clusters is higher than the total number of classes, the extra clusters are assigned to the null set, and all instances assigned to those clusters are said to have been predicted incorrectly. Conversely, if the number of clusters is lower than the number of classes, extra classes are assigned to the null set, and all instances with those ground truth labels are said to have been to be predicted incorrectly. Thus, we assume that, if the clustering (across \mathcal{D}) is performed with k too high or too low, then this will be reflected in a sub-optimal clustering accuracy on $\mathcal{D}_{\mathcal{L}}$. In other words, we assume clustering accuracy on the labelled set will be maximized when $k = |\mathcal{Y}_{\mathcal{L}} \cup \mathcal{Y}_{\mathcal{U}}|$. This intuition leads us to use the clustering accuracy as a 'black box' scoring function, $ACC = f(k; \mathcal{D})$, which we optimize with Brent's algorithm to find the optimal k .

3.3. Two strong baselines

To the best of our knowledge, there is no baseline for GCD that can be used as-is from the literature. Instead, we adapt two NCD baselines for it: RankStats [16], which is widely used as a competitive baseline for novel category discovery, and UNO [12], which is to the best of our knowledge the state-of-the-art method for NCD.

Baseline: RankStats+ RankStats trains two classifiers on top of a shared feature representation: the first head is fed instances from the labelled set and is trained with the cross-entropy loss, while the second head sees only instances from unlabelled classes (again, in the NCD setting, the labelled and unlabelled classes are disjoint). In order to adapt RankStats to GCD, we train it with a single classification head for the total number of classes in the dataset. We then train the first $|\mathcal{Y}_L|$ elements of the head with the cross-entropy loss, and train the *entire* head with the binary cross-entropy loss with pseudo-labels.

Baseline: UNO+ Similarly to RankStats, UNO is trained with classification heads for labelled and unlabelled data. The model is then trained in a SwAV-like manner [4]. First, multiple views (random augmentations) of a batch are generated and fed to the same model. For the labelled images in the batch, the labelled head is trained with the cross-entropy loss using the ground truth labels. For the unlabelled images, predictions (logits from the unlabelled head) are gathered for a given view and used as pseudo-labels with which to optimize the loss from *other* views. To adapt this mechanism, we simply concatenate both the labelled and unlabelled heads, thus allowing generated pseudo-labels for the unlabelled samples to belong to any class in the dataset.

4. Experiments

4.1. Experimental setup

Data We demonstrate results on six datasets in our proposed setting. For each dataset, we take the training set and sample a set of classes for which we have labels during training. We further sub-sample 50% of the images from these classes to constitute the labelled set \mathcal{D}_L . The remaining instances from these classes, along with all instances from the other classes, constitute \mathcal{D}_U . We further construct the validation set for the labelled classes from the test or validation split of each dataset.

We first demonstrate results on three generic object recognition datasets: CIFAR10 [25], CIFAR100 [25] and ImageNet-100 [9]. ImageNet-100 refers to the ImageNet dataset with 100 classes randomly subsampled. These datasets establish the methods’ ability to identify categories with abstract class definitions, as may be encountered in settings such as self-driving or animal monitoring in the wild.

We further demonstrate results on three fine-grained

Table 1. Datasets used in our experiments. We show the number of classes in the labelled and unlabelled sets ($|\mathcal{Y}_L|$, $|\mathcal{Y}_U|$), as well as the number of images ($|\mathcal{D}_L|$, $|\mathcal{D}_U|$).

	CIFAR10	CIFAR100	ImageNet-100	CUB	SCars	Herb19
$ \mathcal{Y}_L $	5	80	50	100	98	341
$ \mathcal{Y}_U $	10	100	100	200	196	683
$ \mathcal{D}_L $	12.5k	20k	31.9k	1.5k	2.0k	8.9k
$ \mathcal{D}_U $	37.5k	30k	95.3k	4.5k	6.1k	25.4k

datasets: CUB [43], Stanford Cars [24] and Herbarium19 [39]. Recent work has identified the need for open-set benchmarks which have a clearly defined concept of a ‘semantic class’ [42], proposing fine-grained visual categorization (FGVC) datasets as a solution to this. In these benchmarks, there are specific ‘axes of semantic variation’ — e.g., the difference between two bird species in CUB vs. the difference between a dog and a refrigerator in ImageNet. Thus, the user can be more confident that the recognition system is identifying new classes based on a true semantic signal, rather than simply responding to low-level distributional shifts in the data, as may be the case for generic object recognition datasets. The long-tailed nature of Herbarium19 adds an additional dimension to the evaluation.

FGVC datasets further reflect a number of real-world use cases for image recognition systems, which are deployed in constrained environments with many similar objects (e.g. products in a supermarket). In fact, the Herbarium19 dataset itself represents a real-world use case for GCD: while we are aware of roughly 400k species of plants, and estimate that there are around 80k yet to be discovered, it currently takes roughly 35 years from plant collection to plant species description if performed manually [39]. We summarise the dataset splits used in our evaluations in Tab. 1, and provide more details in Appendix A.

Evaluation protocol For each dataset, we train the models on \mathcal{D} (without access to the ground truth labels in \mathcal{D}_U). At test-time, we measure the clustering accuracy between the ground truth labels y_i and the model’s predictions \hat{y}_i as:

$$ACC = \max_{p \in \mathcal{P}(\mathcal{Y}_U)} \frac{1}{M} \sum_{i=1}^M \mathbb{1}\{y_i = p(\hat{y}_i)\} \quad (4)$$

Here, $M = |\mathcal{D}_U|$ and $\mathcal{P}(\mathcal{Y}_U)$ is the set of all permutations of the class labels in the unlabelled set. The maximum over the set of permutations is computed via the Hungarian optimal assignment algorithm [26].

Implementation details All methods are trained with a ViT-B-16 backbone with DINO pre-trained weights, and use the output [CLS] token as the feature representation. All methods were trained for 200 epochs, or until convergence as defined by the accuracy on the validation set.

For our method, we fine-tune the final block of the vision transformer with an initial learning rate of 0.1 which we

decay with a cosine annealed schedule. We use a batch size of 128 and $\lambda = 0.35$ in the loss (see Eq. (3)). Furthermore, following standard practise in self-supervised learning, we project the model’s output through a non-linear projection head before applying the contrastive loss. We use the same projection head as in [5] and discard it at test-time.

For the baselines from NCD, we follow the original implementations and learning schedules as far as possible, referring to the original papers for details [12, 16]. For these experiments, we freeze the backbone and train only the classification heads. We also experimented with fine-tuning different amounts of the backbone, but found that a frozen backbone worked best for the baseline methods. Finally, we also experimented with training a lightweight (ResNet-18) backbone from scratch for this task, and also ensured that our implementations could recreate the reported figures in the original NCD setting.

Finally, in order to estimate k , we run our k -estimation method on DINO features extracted from each of the considered benchmarks. We run Brent’s algorithm on a constrained domain for k , with the minimum set at $|\mathcal{Y}_L|$ and the maximum set at 1000 classes for all datasets.

4.2. Comparison with the baselines

We report results for all compared methods in Tab. 2 and Tab. 3. As an additional baseline, we also report results when running k -means directly on top of raw DINO features (reported as k -means). We report ACC values for both the ‘Old’ classes (instances in \mathcal{D}_U belonging to classes in \mathcal{Y}_L) and ‘New’ classes (instances in \mathcal{D}_U belonging to classes in $\mathcal{Y}_U \setminus \mathcal{Y}_L$). Finally, we report the aggregated accuracy, ‘All’, over all instances in \mathcal{D}_U .

The results on the generic object recognition datasets are presented in Tab. 2. We note that, on all datasets, the best performance aggregated over the entire unlabelled set is achieved by our method. Our model further outperforms the baselines in most subcategories of the datasets. The exception is ImageNet-100, where raw DINO features perform better on the ‘New’ classes (with no labels available in \mathcal{D}) and UNO+ performs better on the ‘Old’ ones (from the same classes as those in \mathcal{D}_L). The first result is explained as DINO is trained in a self-supervised manner on the entire ImageNet dataset, where it has been carefully tuned to achieve a strong representation for all classes. We suggest that the second result is due to ImageNet-100 containing many classes, but also containing enough images (≈ 650) per class to reliably train a linear classifier with cross-entropy. In this regime, in the supervised setting, it is still difficult to beat a standard classification head. Nonetheless, the best tradeoff between the ‘New’ and ‘Old’ classes is still achieved by our approach. We also note that the methods based on parametric classifiers show a substantial discrepancy between their performances on the ‘Old’

and ‘New’ classes, demonstrating overfitting on the labelled categories. Across ‘All’ classes in Tab. 2, on average, our method outperforms the nearest baseline by 6.9% in absolute terms, and by 9.6% in proportional terms.

The results on the FGVC datasets are shown in Tab. 3. In this more challenging setting, our approach outperforms the baselines substantially in all cases except for the ‘Old’ classes in Herbarium19. In this case, RankStats+ demonstrates strong performance, though it once again overfits to the ‘Old’ classes and underperforms our method significantly over ‘All’ classes. On the FGVC datasets, we find our method outperforms the nearest baseline by 11.6% on average in absolute terms, and 34.7% in proportional terms.

Table 2. Results on generic image recognition datasets.

Classes	CIFAR10			CIFAR100			ImageNet-100		
	All	Old	New	All	Old	New	All	Old	New
k -means [28]	83.6	85.7	82.5	52.0	53.7	51.1	73.4	75.5	71.3
RankStats+	84.5	96.4	78.5	65.0	78.8	37.4	50.9	94.2	29.2
UNO+	72.4	95.0	61.1	64.1	73.8	44.8	62.3	94.7	46.0
Ours	91.5	97.9	88.2	76.9	84.5	61.7	75.1	92.2	66.5

Table 3. Results on fine-grained image recognition datasets.

Classes	CUB			Stanford Cars			Herbarium19		
	All	Old	New	All	Old	New	All	Old	New
k -means [28]	35.7	42.3	32.4	14.2	14.2	14.2	14.1	14.7	13.3
RankStats+	37.1	73.8	18.7	29.2	53.6	17.1	31.4	54.5	18.9
UNO+	40.1	71.1	24.5	20.6	33.7	14.1	21.2	36.1	13.3
Ours	54.0	75.4	43.4	42.0	61.2	32.4	39.4	40.5	38.5

4.3. Estimating the number of classes

We report results on estimating the number of classes in Tab. 4. We find that on the generic object recognition datasets, we can come very close to the ground truth number of categories in the unlabelled set, with a maximum error of 10%. On the FGVC datasets, we report an average discrepancy of 18.9%. We note the highly challenging nature of the FGVC datasets, with many constituent classes which are visually similar.

4.4. Ablation study

In Tab. 5, we inspect the contributions of the various elements of our proposed approach. Specifically, we identify the importance of the following components of the method: ViT backbone; contrastive fine-tuning (regular and supervised); and semi-supervised k -means clustering.

ViT Backbone Rows (1) and (2) show the effect of the ViT model for the clustering task, as (1) and (2) represent

Table 4. Estimation of the number of classes in unlabelled data.

	CIFAR10	CIFAR100	ImageNet-100	CUB	SCars	Herb19
Ground truth	10	100	100	200	196	683
Ours	9	100	109	231	230	520
Error	10%	0%	9%	16%	15%	28%

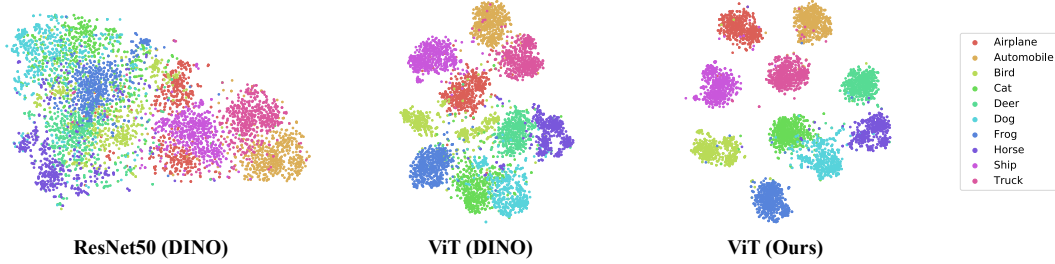


Figure 2. TSNE visualization of instances in CIFAR10 for features generated by a ResNet-50 and ViT model trained with DINO self-supervision on ImageNet, and a ViT model after fine-tuning with our approach.

Table 5. Ablation study on the different components of our approach.

	ViT Backbone	Contrastive Loss	Sup. Contrastive Loss	Semi-Sup k -means	CIFAR100			Herbarium19		
					All	Old	New	All	Old	New
(1)	✗	✗	✗	✗	34.0	34.8	32.4	12.1	12.5	11.9
(2)	✓	✗	✗	✗	52.0	53.7	51.1	14.1	14.7	13.3
(3)	✓	✓	✗	✗	54.6	54.1	53.7	14.3	15.1	13.9
(4)	✓	✗	✓	✗	60.5	72.2	35.0	17.8	22.7	15.4
(5)	✓	✓	✓	✗	74.5	81.2	61.2	30.5	35.3	27.9
(6)	✓	✓	✓	✓	76.9	84.5	61.7	39.4	40.5	38.5

a ResNet-50 model and ViT-B-16 trained with DINO respectively. The ResNet model performs nearly 20% worse aggregated over ‘Old’ and ‘New’ classes. To disambiguate this from the general capacity of the architecture, note that the ImageNet linear probe discrepancy (the standard evaluation protocol for self-supervised models) is roughly 3% [5]. Meanwhile, the discrepancy in their k -NN accuracies on ImageNet is roughly 9% [5], suggesting why the ViT model performs so much better for the clustering task.

Contrastive fine-tuning Rows (2)-(5) show the effects of introducing different combinations of contrastive fine-tuning on the target dataset. We find that including any of the contrastive methods alone gives relatively marginal improvements over using the raw DINO features. We find that the full benefit is only realized when combining the self-supervised and supervised contrastive losses on the target dataset. Specifically, the combination of the contrastive losses allows us to boost aggregated clustering accuracy by a further 23% on CIFAR100 and by 16% on Herbarium19 (more than doubling the ACC in this case).

Semi-supervised k -means The semi-supervised clustering also improves ACC across the board. In general, we found that semi-supervised clustering was beneficial on all datasets, and gave a particular boost on the FGVC benchmarks. For instance, in the Herbarium19 case, it improves aggregated ACC by nearly 10%.

Summary Overall, we find that none of the components of our method are individually sufficient to achieve good performance across our benchmark datasets. Specifically, the *combination* of a vision transformer backbone and contrastive fine-tuning facilitates strong k -means cluster-

ing directly in the feature space of the model. The semi-supervised k -means algorithm further allows us to guide the clustering process with labels and achieve better ACC , especially on the fine-grained datasets.

We further illustrate this point in the TSNE visualizations in Fig. 2, performed on the CIFAR10 dataset. We show TSNE projections of raw ResNet-50 and ViT DINO features, as well as those of our model. For the ResNet-50 features, points from the same class are generally projected close to each other, indicating that they are likely to be separable given a simple transformation (*e.g.* a linear probe). However, they do not form clear clusters, hinting at these features’ poor down-stream clustering performance. In contrast, the ViT features form far clearer clusters, which are further distinguished when trained with our approach.

4.5. Qualitative results

Finally, we visualize the attention mechanism of our model to better understand its performance. Specifically, in Fig. 3 we look at how the final multi-head attention layer attends to different spatial locations when supporting the output [CLS] token (which we use as our feature representation). We show this both for the pre-trained DINO model and after training with our method. We visualize the attention maps for images from the ‘Old’ and ‘New’ classes for Stanford Cars and CUB.

It is demonstrated in [5] that different attention heads in the DINO model focus on different regions of an image, without the need for human annotation. We find this to be the case, with different heads attending to disjoint regions of the image and typically focusing on important parts. However, after training with our method, we find heads to be



Figure 3. Attention visualizations for the DINO-ViT model before (left) and after (right) fine-tuning with our approach. For Stanford Cars and CUB, we show an image from the ‘Old’ (first row for each dataset) and ‘New’ classes (second row for each dataset). Our model learns to specialize attention heads (shown as columns) to different semantically meaningful parts, which can transfer between the labelled and unlabelled categories. The model’s heads learn ‘Windshield’, ‘Headlight’ and ‘Wheelhouse’ for the cars, and ‘Beak’, ‘Head’ and ‘Belly’ for the birds. For both models, we select heads with as focused attention as possible. Recommended viewing in color with zoom.

more specialised to semantic parts, displaying more concentrated and local attention. In this way, we suggest the model learns to attend to a set of parts which are transferable between the ‘Old’ and ‘New’ classes, which allows it to better generalize knowledge from the labelled data.

5. Broader impact and limitations

Our method assigns labels to images in an unsupervised manner, including discovering new labels. Even more than standard image classification methods, it should be used with care (e.g., by manually checking the results) in sensitive contexts, such as processing personal data.

We also note some practical limitations. First, we assume that there is no domain shift between the labelled and unlabelled subsets. For instance, we are not tackling the problem of a single model reliably classifying photographs and paintings of the same classes. Second, we do not con-

sider the streaming setting (also known as continual learning): one would need to re-train the model from scratch as new data becomes available.

As for the data used in the experiments, we use standard third-party datasets in a manner compatible with their licenses. Some of these datasets contain Internet images that feature, often incidentally, people — see [2, 32, 44] for an in-depth discussion of the privacy implications.

6. Conclusions

We have proposed and investigated GCD, a more general, challenging and realistic variant of NCD. Given a dataset with partial labels for images and classes, the task is to find the assignment for all unlabelled images, while discovering any new classes. We have developed baselines for the task by transferring state-of-the-art algorithms from NCD and further developed a simple but effective algorithm

which substantially outperforms these baselines. We also proposed a method for identifying the number of categories in the unlabelled data, which is an understudied problem of practical significance. We hope that this work can serve as a foundation from which to tackle this important problem.

References

- [1] David Arthur and Sergei Vassilvitskii. k-means++: the advantages of careful seeding. In *ACM-SIAM symposium on Discrete algorithms*, 2007. 4
- [2] Yuki M. Asano, Christian Rupprecht, Andrew Zisserman, and Andrea Vedaldi. PASS: An ImageNet replacement for self-supervised pretraining without human. *NeurIPS Track on Datasets and Benchmarks*, 2021. 8
- [3] Abhijit Bendale and Terrance E. Boult. Towards open set deep networks. In *CVPR*, 2016. 2
- [4] Mathilde Caron, Ishan Misra, Julien Mairal, Priya Goyal, Piotr Bojanowski, and Armand Joulin. Unsupervised learning of visual features by contrasting cluster assignments. In *NeurIPS*, 2020. 5
- [5] Mathilde Caron, Hugo Touvron, Ishan Misra, Hervé Jégou, Julien Mairal, Piotr Bojanowski, and Armand Joulin. Emerging properties in self-supervised vision transformers. In *ICCV*, 2021. 3, 6, 7
- [6] Olivier Chapelle, Bernhard Scholkopf, and Alexander Zien. *Semi-Supervised Learning*. MIT Press, 2006. 2
- [7] Guangyao Chen, Peixi Peng, Xiangqian Wang, and Yonghong Tian. Adversarial reciprocal points learning for open set recognition. *IEEE TPAMI*, 2021. 2
- [8] Guangyao Chen, Limeng Qiao, Yemin Shi, Peixi Peng, Jia Li, Tiejun Huang, Shiliang Pu, and Yonghong Tian. Learning open set network with discriminative reciprocal points. In *ECCV*, 2020. 2
- [9] Jia Deng, Wei Dong, Richard Socher, Li-Jia Li, Kai Li, and Li Fei-Fei. Imagenet: A large-scale hierarchical image database. In *CVPR*, 2009. 3, 5
- [10] Alexey Dosovitskiy, Lucas Beyer, Alexander Kolesnikov, Dirk Weissenborn, Xiaohua Zhai, Thomas Unterthiner, Mostafa Dehghani, Matthias Minderer, Georg Heigold, Sylvain Gelly, Jakob Uszkoreit, and Neil Houlsby. An image is worth 16x16 words: Transformers for image recognition at scale. In *ICLR*, 2021. 3
- [11] Lei Feng, Senlin Shu, Zhuoyi Lin, Fengmao Lv, Li Li, and Bo An. Can cross entropy loss be robust to label noise? In *IJCAI*, 2020. 3
- [12] Enrico Fini, Enver Sangineto, Stéphane Lathuilière, Zhun Zhong, Moin Nabi, and Elisa Ricci. A unified objective for novel class discovery. In *ICCV*, 2021. 3, 5, 6
- [13] Zongyuan Ge, Sergey Demyanov, and Rahil Garnavi. Generative openmax for multi-class open set classification. In *BMVC*, 2017. 2
- [14] Michael Gutmann and Aapo Hyvärinen. Noise-contrastive estimation: A new estimation principle for unnormalized statistical models. In *Proceedings of the Thirteenth International Conference on Artificial Intelligence and Statistics*, 2010. 3
- [15] Kai Han, Sylvestre-Alvise Rebuffi, Sebastien Ehrhardt, Andrea Vedaldi, and Andrew Zisserman. Automatically discovering and learning new visual categories with ranking statistics. In *ICLR*, 2020. 3
- [16] Kai Han, Sylvestre-Alvise Rebuffi, Sebastien Ehrhardt, Andrea Vedaldi, and Andrew Zisserman. Autonovel: Automatically discovering and learning novel visual categories. *IEEE TPAMI*, 2021. 3, 5, 6
- [17] Kai Han, Andrea Vedaldi, and Andrew Zisserman. Learning to discover novel visual categories via deep transfer clustering. In *ICCV*, 2019. 2, 3
- [18] Kaiming He, Xiangyu Zhang, Shaoqing Ren, and Jian Sun. Deep residual learning for image recognition. In *CVPR*, 2016. 4
- [19] Yen-Chang Hsu, Zhaoyang Lv, and Zsolt Kira. Learning to cluster in order to transfer across domains and tasks. In *ICLR*, 2018. 3
- [20] Yen-Chang Hsu, Zhaoyang Lv, Joel Schlosser, Phillip Odom, and Zsolt Kira. Multi-class classification without multi-class labels. In *ICLR*, 2019. 3
- [21] Xuhui Jia, Kai Han, Yukun Zhu, and Bradley Green. Joint representation learning and novel category discovery on single- and multi-modal data. In *ICCV*, 2021. 3
- [22] Prannay Khosla, Piotr Teterwak, Chen Wang, Aaron Sarna, Yonglong Tian, Phillip Isola, Aaron Maschinot, Ce Liu, and Dilip Krishnan. Supervised contrastive learning. *arXiv preprint arXiv:2004.11362*, 2020. 3
- [23] Shu Kong and Deva Ramanan. Opengan: Open-set recognition via open data generation. *ICCV*, 2021. 2
- [24] Jonathan Krause, Michael Stark, Jia Deng, and Li Fei-Fei. 3d object representations for fine-grained categorization. In *4th International IEEE Workshop on 3D Representation and Recognition (3dRR-13)*, 2013. 5
- [25] Alex Krizhevsky and Geoffrey Hinton. Learning multiple layers of features from tiny images. *Technical report*, 2009. 5
- [26] Harold W Kuhn. The hungarian method for the assignment problem. *Naval research logistics quarterly*, 1955. 4, 5
- [27] Samuli Laine and Timo Aila. Temporal ensembling for semi-supervised learning. In *ICLR*, 2017. 2
- [28] James MacQueen. Some methods for classification and analysis of multivariate observations. In *Proceedings of the Fifth Berkeley Symposium on Mathematical Statistics and Probability*, 1967. 6
- [29] Lawrence Neal, Matthew Olson, Xiaoli Fern, Weng-Keen Wong, and Fuxin Li. Open set learning with counterfactual images. In *ECCV*, 2018. 2
- [30] Avital Oliver, Augustus Odena, Colin Raffel, Ekin D. Cubuk, and Ian J. Goodfellow. Realistic evaluation of deep semi-supervised learning algorithms. In *NeurIPS*, 2018. 2
- [31] Poojan Oza and Vishal M. Patel. C2ae: Class conditioned auto-encoder for open-set recognition. In *CVPR*, 2019. 2
- [32] Vinay Uday Prabhu and Abeba Birhane. Large image datasets: A pyrrhic win for computer vision? In *Proc. WACV*, 2020. 8
- [33] Antti Rasmus, Harri Valpola, Mikko Honkala, Mathias Berglund, and Tapani Raiko. Semi-supervised learning with ladder networks. In *NeurIPS*, 2015. 2

- [34] Sylvestre-Alvise Rebuffi, Sebastien Ehrhardt, Kai Han, Andrea Vedaldi, and Andrew Zisserman. Semi-supervised learning with scarce annotations. *arxiv*, 2019. 2
- [35] Walter J. Scheirer, Anderson Rocha, Archana Sapkota, and Terrance E. Boult. Towards open set recognition. *IEEE TPAMI*, 2013. 2
- [36] Yu Shu, Yemin Shi, Yaowei Wang, Tiejun Huang, and Yonghong Tian. P-odn: Prototype-based open deep network for open set recognition. *Scientific Reports*, 2020. 2
- [37] Kihyuk Sohn, David Berthelot, Chun-Liang Li, Zizhao Zhang, Nicholas Carlini, Ekin D. Cubuk, Alex Kurakin, Han Zhang, and Colin Raffel. Fixmatch: Simplifying semi-supervised learning with consistency and confidence. In *NeurIPS*, 2020. 2
- [38] Xin Sun, Zhenning Yang, Chi Zhang, Guohao Peng, and Keck-Voon Ling. Conditional gaussian distribution learning for open set recognition. In *CVPR*, 2020. 2
- [39] Kiat Chuan Tan, Yulong Liu, Barbara Ambrose, Melissa Tulig, and Serge Belongie. The herbarium challenge 2019 dataset. In *Workshop on Fine-Grained Visual Categorization*, 2019. 5
- [40] Antti Tarvainen and Harri Valpola. Mean teachers are better role models: Weight-averaged consistency targets improve semi-supervised deep learning results. In *NeurIPS*, 2017. 2
- [41] Ashish Vaswani, Noam Shazeer, Niki Parmar, Jakob Uszkoreit, Llion Jones, Aidan N Gomez, Łukasz Kaiser, and Illia Polosukhin. Attention is all you need. In *NeurIPS*, 2017. 2
- [42] Sagar Vaze, Kai Han, Andrea Vedaldi, and Andrew Zisserman. Open-set recognition: A good closed-set classifier is all you need. *arXiv preprint arXiv:2110.06207*, 2021. 3, 5
- [43] Catherine Wah, Steve Branson, Peter Welinder, Pietro Perona, and Serge Belongie. The caltech-ucsd birds-200-2011 dataset. *Technical Report CNS-TR-2011-001, California Institute of Technology*, 2011. 5
- [44] Kaiyu Yang, Jacqueline Yau, Li Fei-Fei, Jia Deng, and Olga Russakovsky. A study of face obfuscation in imagenet. *CoRR*, abs/2103.06191, 2021. 8
- [45] Ryota Yoshihashi, Wen Shao, Rei Kawakami, Shaodi You, Makoto Iida, and Takeshi Naemura. Classification-reconstruction learning for open-set recognition. In *CVPR*, 2019. 2
- [46] Xiaohua Zhai, Avital Oliver, Alexander Kolesnikov, and Lucas Beyer. S4l: Self-supervised semi-supervised learning. In *ICCV*, 2019. 2
- [47] Hongjie Zhang, Ang Li, Jie Guo, and Yanwen Guo. Hybrid models for open set recognition. In *ECCV*, 2020. 2
- [48] Bingchen Zhao and Kai Han. Novel visual category discovery with dual ranking statistics and mutual knowledge distillation. In *NeurIPS*, 2021. 3
- [49] Zhun Zhong, Enrico Fini, Subhankar Roy, Zhiming Luo, Elisa Ricci, and Nicu Sebe. Neighborhood contrastive learning for novel class discovery. In *CVPR*, 2021. 3
- [50] Zhun Zhong, Linchao Zhu, Zhiming Luo, Shaozi Li, Yi Yang, and Nicu Sebe. Openmix: Reviving known knowledge for discovering novel visual categories in an open world. In *CVPR*, 2021. 3

Generalized Category Discovery

Appendices

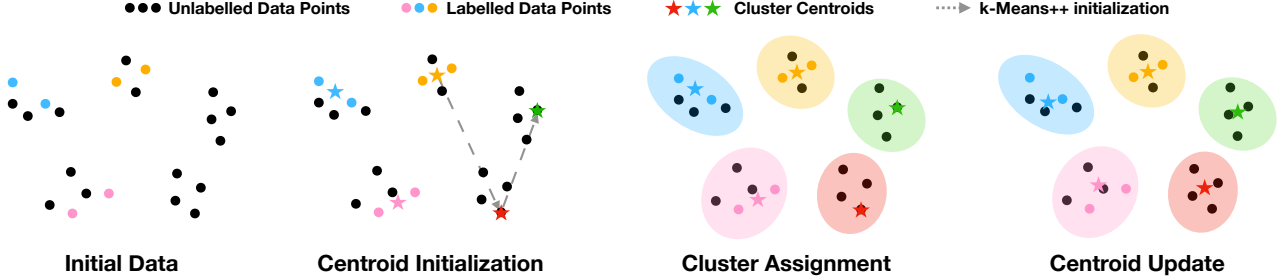


Figure 4. **Semi-supervised k -means algorithm shown for $k = 5$.** Given partially labelled data points (Initial Data), we first initialize $|\mathcal{Y}_{\mathcal{L}}| = 3$ centroids by the average of labelled data points in each labelled class (shown as colored dots). Starting from these centroids, we run k -means++ (dashed arrows) on the unlabelled data (black dots) to further obtain $|\mathcal{Y}_{\mathcal{U}} \setminus \mathcal{Y}_{\mathcal{L}}| = 2$ centroids (Centroid Initialization). Having obtained $k = 5$ centroids (colored stars), we assign each data point a cluster label by identifying its nearest centroid (Cluster Assignment), after which we can update the centroids by averaging all data points in each cluster (Centroid Update). We repeat the cycle of Cluster Assignment and Centroid Update iteratively, until the k -means algorithm converges. During each cycle, we force the labelled data points to follow their ground-truth label, *i.e.* all labelled points of the same class fall into the same cluster.

A. Dataset details

Here, we describe which classes constitute the ‘Old’ and ‘New’ categories in the Generalized Category Discovery setting, for each dataset used in this paper.

For all datasets, we sample 50% of the classes as ‘Old’ classes ($\mathcal{Y}_{\mathcal{L}}$) and keep the rest as ‘New’ ($\mathcal{Y}_{\mathcal{U}} \setminus \mathcal{Y}_{\mathcal{L}}$). For all datasets, *except for Herbarium19*, we use the first 50% of classes (according to their class index) in $\mathcal{Y}_{\mathcal{L}}$. For Herbarium19, to account for the long-tailed nature of the dataset, we randomly sample the ‘Old’ classes from the total list of classes. Further details on the splits can be found in Tab. 1 in the main paper.

B. Semi-supervised k -means

We elaborate on the semi-supervised k -means algorithm for GCD (from Sec. 3.1.2 of the main paper) in Fig. 4.

C. Estimating the number of classes

In Fig. 5, we provide motivation for our algorithm in Sec. 3.2 of the main paper, which is used to estimate the number of classes in the dataset ($k = |\mathcal{Y}_{\mathcal{L}} \cup \mathcal{Y}_{\mathcal{U}}|$).¹

Specifically, we plot how the clustering accuracy on the labelled subset ($\mathcal{D}_{\mathcal{L}}$) changes as we run k -means with varying k on the entire dataset ($\mathcal{D}_{\mathcal{L}} \cup \mathcal{D}_{\mathcal{U}}$), for a range of datasets. It can be seen that the *ACC* on the labelled subset follows an approximately bell-shaped function for all datasets. Furthermore, the function is maximized when k -means clustering is run with roughly the ground truth number of classes

¹Note that $|\mathcal{Y}_{\mathcal{L}} \cup \mathcal{Y}_{\mathcal{U}}| = |\mathcal{Y}_{\mathcal{U}}|$ as $|\mathcal{Y}_{\mathcal{L}}| \subset |\mathcal{Y}_{\mathcal{U}}|$. We use the former notation for clarity.

for each dataset, indicating that optimizing for this maximum is a reasonable way of identifying the total number of categories.

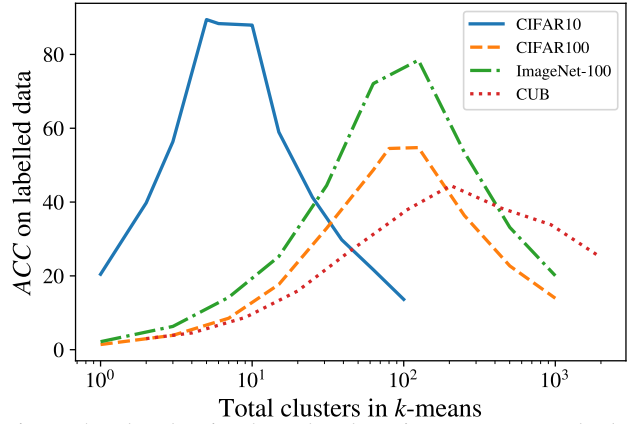


Figure 5. Plot showing how the clustering accuracy on the labelled subset ($\mathcal{D}_{\mathcal{L}}$) changes as we run k -means, with varying k , on the *entire* dataset ($\mathcal{D}_{\mathcal{L}} \cup \mathcal{D}_{\mathcal{U}}$). The ground-truth number of classes in CIFAR10, CIFAR100, ImageNet-100 and CUB are [10, 100, 100, 200] respectively.

D. Attention maps

Here, we expand upon the attention visualizations from Fig. 3. We first describe the process for constructing them, before providing further examples in Fig. 6.

Visualization construction: The attention visualizations were constructed by considering how different attention heads, supporting the output [CLS] token, attended to dif-

ferent spatial locations. Specifically, consider the input to the final block of the ViT model, $\mathbf{X} \in \mathbb{R}^{(HW+1) \times D}$, corresponding to a feature for each of the HW patches fed to the model, plus a feature corresponding to the $[\text{CLS}]$ token. Here, $HW = 14 \times 14 = 196$ patches at resolution 16×16 pixels. These features are passed to a multi-head self-attention ($MHSA$) layer which can be described as:

$$MHSA(\mathbf{X}) = [\text{head}_1, \dots, \text{head}_h] \mathbf{W}_0, \quad (5)$$

where

$$\text{head}_j = \text{Attention}(\mathbf{XW}_j^Q, \mathbf{XW}_j^K, \mathbf{XW}_j^V). \quad (6)$$

In other words, the layer comprises several attention heads ($h = 12$ in the ViT model) which each independently attend over the input features to the block. We refer to [41] for more details on the self-attention mechanism. We note that, for each feature $i \in \mathbf{X}$, an attention vector is generated for each head j , as $A_{ij} \in [0, 1]^{HW+1}$ to describe how every head j relates each feature to every other feature.

We look at only the attention values for the $[\text{CLS}]$ token, A_{0j} , and further only look at the elements which attend to spatial locations. We find that, while some heads have uninterpretable attention maps, certain heads specialize to attend to coherent semantic object parts.

Discussion on attention visualizations We provide further attention visualizations in Fig. 6. We show the *same* attention heads as shown in Fig. 3 (both for models trained with our method and for the original DINO model).

We first note that the DINO features often attend to salient object regions. For instance, ‘Head 1’ of the model often focuses on the wheel of the car (in the Stanford Cars examples), while ‘Head 2’ of the model generally attends to the heads of the birds (in the CUB examples). Overall, however, with the pre-trained DINO model, there is relatively little semantic consistency between the attention maps of a given head (*i.e.* within columns for each dataset).

In contrast, we find that the models trained with our approach specialize attention heads in semantically meaningful ways. The heads shown correspond to ‘Windshield’, ‘Headlight’ and ‘Wheelhouse’ for the Stanford Cars model, and ‘Beak’, ‘Head’ and ‘Belly’ for the CUB model. We find these maps to be relatively robust to nuisance factors such as pose and scale shift, as well as distracting objects in the image. We note a failure case (rightmost image, Row 2), as the ‘Wheelhouse’ attention head is forced to attend to miscellaneous regions of the car, as the car’s wheelhouse is not visible in this image.

The ability of the model to identify and distinguish different semantic parts of an object is useful for the GCD task. Particularly in the fine-grained setting, the constituent set of parts of an object (‘Head’, ‘Beak’, ‘Belly’ *etc.* for the birds)

transfer between ‘Old’ and ‘New’ classes. Thus, we suggest that the attention mechanism of the model allows it to generalize its understanding from the labelled ‘Old’ classes, and apply it to the unlabelled ‘New’ ones.



Figure 6. **Attention visualizations.** Attention maps for the DINO model before (left) and after (right) fine-tuning with our approach on the Stanford Cars (top) and CUB (bottom) datasets. For each dataset, we show two rows of images from the ‘Old’ classes (solid green box) and two rows of images from the ‘New’ classes (dashed red box). Our model learns to specialize attention heads (shown as columns) to different semantically meaningful object parts, which can transfer between the ‘Old’ and ‘New’ categories.